



RESEARCH ARTICLE

10.1002/2016WR020354

Special Section:

Engagement, Communication, and Decision-Making Under Uncertainty

Key Points:

- Decisions on adaptation measures need to take careful account of all uncertainties
- Modeling local sea level rise is essential
- Decisions under uncertainty do not have to be based on precise damage costs

Correspondence to:

T. L. Thorarinsdottir,
thordis@nr.no

Citation:

Thorarinsdottir, T. L., P. Guttorp, M. Drews, P. Skougaard Kaspersen, and K. de Bruin (2017), Sea level adaptation decisions under uncertainty, *Water Resour. Res.*, 53, 8147–8163, doi:10.1002/2016WR020354.



Received 31 DEC 2016

Accepted 14 AUG 2017

Accepted article online 21 AUG 2017

Published online 8 OCT 2017

Sea level adaptation decisions under uncertainty

T. L. Thorarinsdottir¹ , P. Guttorp¹, M. Drews², P. Skougaard Kaspersen², and K. de Bruin^{3,4} 

¹Norwegian Computing Center, Oslo, Norway, ²Technical University of Denmark, Copenhagen, Denmark, ³Center for International Climate and Environmental Research, Oslo, Norway, ⁴Wageningen Environmental Research, Wageningen, Netherlands

Abstract

Sea level rise has serious consequences for harbor infrastructure, storm drains and sewer systems, and many other issues. Adapting to sea level rise requires comparing different possible adaptation strategies, comparing the cost of different actions (including no action), and assessing where and at what point in time the chosen strategy should be implemented. All these decisions must be made under considerable uncertainty—in the amount of sea level rise, in the cost and prioritization of adaptation actions, and in the implications of no action. Here we develop two illustrative examples: for Bergen on Norway's west coast and for Esbjerg on the west coast of Denmark, to highlight how technical efforts to understand and quantify uncertainties in hydrologic projections can be coupled with concrete decision-problems framed by the needs of the end-users using statistical formulations. Different components of uncertainty are visualized. We demonstrate the value of uncertainties and show for example that failing to take uncertainty into account can result in the median-projected damage costs being an order of magnitude smaller.

1. Introduction

The potential impact of climate change on local sea level, yielding effects such as frequent flooding, inundation and backflow of storm drainage and sewer systems, destructive erosion, and contamination of wetlands and other habitats, requires city planners to make decisions in the presence of substantial uncertainty.

As adaptation decision-making is an ongoing process of weighing and choosing which measures should be taken at which moment in time [Hallegatte *et al.*, 2012], adaptive planning methods need to support decisions in the short term, while considering long-term developments. Challenges of adaptation decision-making under uncertainty relate to the incorporation of spatial, intertemporal, and flexibility aspects of adaptation priorities [Fankhauser and Soare, 2013] and the linkage with specific characteristics of sectors and contexts [Bisaro *et al.*, 2016; Hinkel and Bisaro, 2016]. Several economic decision support tools and methods exist for adaptation assessment under uncertainty [e.g., Chambwera *et al.*, 2014; Wilby and Dessai, 2010; Walker *et al.*, 2013]. However, Watkiss *et al.* [2015] conclude that these tools are very resource intensive and complex in the context of long-term adaptation investment decisions and call for the development of “light touch” approaches to better support local adaptation making.

For the adaptation context, light touch decision tools capture elements of decision-making under uncertainty while, as argued by Watkiss *et al.* [2015], keeping a degree of economic rigor. The approach supports local adaptation planners in their adaptation planning processes and evaluation of adaptation options when restricted time, skills, and resources are available [Bisaro *et al.*, 2016]. Also, for example, in the context of groundwater modeling, there is a call for light touch approaches, specially computationally frugal methods that require less model runs, and make it easier to analyze complex models, compare multiple alternative models, and provide insight into models used for computationally demanding assessments of management solutions [Hill *et al.*, 2016].

In April 2016, we organized a workshop where representatives from science and practice discussed the practical and methodological challenges of climate change adaptation [Thorarinsdottir and de Bruin, 2016]. The goal of the workshop was to engage practitioners and scientists in a two-way discussion for an enhanced understanding and transparency between the scientists, the decision-makers, and other practitioners. One of the main conclusions was a call for light touch decision tools. In addition, the participants



Figure 1. Terrain maps of central Bergen, Norway (left) and Esbjerg, Denmark (right).

identified the treatment of uncertainty as one of the main challenges of adaptation decision-making. This included, in particular, the exposure and presentation of uncertainty, and the joint modeling of uncertainty arising from climate projections, impacts, and benefits [de Bruin and Thorarinsdottir, 2016].

The aim of this paper is to address some of these challenges. Specifically, we employ light touch decision tools to demonstrate the importance of combining projections of sea level rise and flood damages alongside a detailed quantification of both hydrologic and economic uncertainties in the context of real-life decision-problems experienced by stakeholders and authorities in two northern European cities, Bergen in Norway, and Esbjerg in Denmark (see Figure 1). Based on communications with local end-users, we highlight the value of taking into account uncertainty through two simplified and complementary case studies, where in the first one planners want to know how early they should implement costly adaptation measures, whereas in the second case the aim is to highlight the risk of flooding in coastal areas, e.g., in order to prioritize future adaptation actions and investments. In both cases we show that embracing the uncertainties derived from economic and hydrologic models are absolutely crucial steps in the decision-making process.

The remainder of the paper is organized as follows. Section 2 describes our approach to projecting sea level change and its uncertainty. In sections 3 and 4 we describe the type of decision-problems that we are going to tackle. We apply these tools to sea level projections for Bergen, Norway and for Esbjerg, Denmark in section 5. In section 6 we demonstrate the consequences of ignoring the uncertainty in the projections, and the paper is closed with conclusions in section 7.

2. Sea Level Projections

We project local sea level changes by modeling two processes, the relationship between global temperature and global sea level and the relationship between global sea level and local sea level.

2.1. Global Sea Level

Most climate models do not explicitly provide sea level as an output of the calculations. Rather, the IPCC AR5 report [Stocker et al., 2013, chap. 13] combines the heat expansion of the ocean with temperature forced models for glacial melt, Greenland ice melt, and Antarctic ice melt and with land rise due to rebound

from the last ice age and other tectonic effects. The uncertainty analysis is a combination of a variety of approaches.

In the present study we use a variant of the empirical approach of Rahmstorf and collaborators [Rahmstorf, 2007; Rahmstorf et al., 2011], employing the statistical modeling of Bolin et al. [2014] to relate global annual mean temperature anomalies to global mean sea level anomalies. We then apply the estimated historical relationship to projected temperatures from the CMIP5 experiment [Taylor et al., 2012] to obtain projected global annual mean sea level, taking into account the uncertainty in the statistical model as well as the spread of the temperature projection ensemble (see section 2.3). For the i th temperature projection T_t^i from the ensemble of projections, we estimate the corresponding global mean sea level as

$$H_t^{gl,j} = \int_{t_0}^t \hat{a}(T_u^i - \hat{T}_0) du + \zeta_t, \tag{1}$$

where \hat{a} and \hat{T}_0 are regression parameters of observed global sea level rise on observed global temperature and ζ_t the integrated time series regression error (see Bolin et al. [2014] for details). Bolin et al. [2014] has compared Rahmstorf's original methodology to the variant used in this study, as well as the effect of using different data sets and concludes that our methodology and choice of data sets yield sea level rise projections and uncertainties similar to those in IPCC AR5 [Stocker et al., 2013].

2.2. Local Sea Level

In order to get from global sea level projections to local ones, it is important to note that sea level rise is not uniform over the globe. Glacial and land ice melting affect the local sea level differently depending on where the melted ice is located.

Another major effect in Fennoscandia is the land rise due to isostatic rebound from the glaciers of the last ice age. Again, we will use historical data to relate global sea level to isostatically corrected local sea level using a time series regression model [Guttorp et al., 2014]. On a centennial timescale the correction can be assumed to be linear in time [Simpson et al., 2014], which implies that the glacial isostatic adjustment (gia) is also linear in time, with slope given by the gia obtained from geological models and/or gps measurements. The local sea level projections are obtained by first relating projected temperature to global sea level, and then relating the global sea level to the local one. Each climate model temperature projection yields a different local sea level projection. The local sea level projection based on the i th climate model for years beyond 2000 is estimated as

$$H_t^{loc,i} + \gamma(t - 2000) = \hat{b}H_t^{gl,j} + \varepsilon_t, \tag{2}$$

where γ is the annual land rise rate, t denotes year, \hat{b} is the regression coefficient relating global to local sea level, and the ε_t are Gaussian time series errors. Details of the methodology may be found in Guttorp et al. [2014].

2.3. Uncertainty Assessment

Following the approach of Guttorp et al. [2014], we assess the uncertainty in the local sea level projections taking into account the variability between the climate projections used, the uncertainties in the regressions of global mean temperature on global mean sea level and of global on local sea level. We express the sea level projection uncertainty in terms of a simultaneous confidence band that is of the intended level for all projection years at the same time, using the approach of Bolin and Lindgren [2015]. This allows us, for example, to get a confidence band for the years when a given sea level rise is obtained.

2.4. Limitations of the Sea Level Projections

The main assumption in using historical relationships in statistical projections of the type used in this paper is that there is no major change in how temperature relates to sea level, globally and locally. Among the factors that may invalidate this approach are changes in water storage on land (in essence removing water from the oceans), excessive siphoning of groundwater (resulting in land subsidence), changes in the rates of glacial and land ice melt, and changes in Earth's gravitational field due to transfer of mass from land ice to ocean water. For example, the rate of ice melt on Greenland may suddenly increase substantially due to intense warming of both air and sea water [Bamber and Aspinall, 2013]. A recent paper [Jevrejeva et al.,

2016] indicates that the upper tails of sea level rise may be substantially higher when taking into account expert assessment of land ice melting. Our current climate models are not able to resolve the ice processes sufficiently to include such so called tipping points into the projections. Also, the IPCC scenarios [van Vuuren et al., 2011] do not include changes in water usage [cf. Konikow, 2011; Wada et al., 2012].

3. Damage Costs and Adaptation Decisions

Climate change adaptation is currently moving from theory to practice with practitioners needing to decide how to begin adapting. This implies an increasing need for detailed economic analysis and appraisal of options [Downing, 2012]. Adaptive decision-making approaches can incorporate various types of uncertainty, including a broad range of climate scenarios [Dittrich et al., 2016]. These methods can be classified as science-first or policy-first approaches. The former type has a “predict-then-act” foundation, which starts with climate projections and impact assessments, not linked to any specific adaptation choices [Jones et al., 2014]. The latter starts out with the formulated adaptation plans, and their functioning is tested against different future projections [Dittrich et al., 2016].

Here we take a policy-first approach where we test a current adaptation plan against different sea level and damage cost projections and the inclusion of different sources of uncertainty, essentially an application of robust decision-making in a simplified manner [Groves and Lempert, 2007]. We focus on what this implies for adaptive management as an iterative and interactive process, especially for the timing of adaptation measures and the implications of including uncertainty. In particular, we employ a probabilistic extension of the framework described by Fankhauser et al. [1999] in which we obtain a probabilistic distribution for the net present value damage in a given year for various adaptation options. The probabilistic distribution is constructed by considering uncertainty in the local sea level projections, in the annual damage costs, and in the effect of changes in sea level on the annual damage costs.

3.1. Effect of Changes in Sea Level on Damage Cost

We are interested in projecting the present value damage cost d_i for year t_i where $i \in \{1, \dots, 85\}$ with $t_1=2016, \dots, t_{85}=2100$. We assume that changes in sea level have a multiplicative effect on d_i such that a positive sea level anomaly (w.r.t. the 1999 baseline as used in the sea level projections above) results in a multiplicative factor greater than one while a negative sea level anomaly results in a multiplicative factor smaller than one compared to the damage cost d_b associated with baseline sea level. The multiplicative factor can be described by a monotonic positive function $g(s_i|\beta)$ of the sea level anomaly s_i with parameter vector β such that $g(s|\beta) > 1$ for $s > 0$ and $g(s|\beta) < 1$ for $s < 0$. In addition, we use a discount rate r_i for $i \in \{1, \dots, 85\}$ to transform the future cost to present value. That is, we set

$$d_i = \frac{g(s_i|\beta) d_b}{\prod_{j<i} (1+r_j)} \tag{3}$$

Hallegatte et al. [2013] estimate an effect function similar to our function g valid in 2050 for $s \in \{0, 0.2, 0.4\}$ for 136 coastal cities worldwide. From the probability of various flood levels in each city and data on assets that are exposed at different flood levels, flood asset losses are estimated for six categories of assets. Assuming that future assets in each city have the same elevation distribution as existing assets, future losses are then estimated using a socioeconomic growth scenario. Here we use their results for 15 European cities: Amsterdam, Athens, Barcelona, Dublin, Glasgow, Hamburg, Helsinki, Copenhagen, Lisbon, London, Marseilles, Naples, Porto, Rotterdam, and Stockholm. To obtain a city-specific effect function for a large range of sea level anomalies, we employ a linear extrapolation as shown in Figure 2. We include uncertainty in the effect function by treating the results for the 15 different cities as an exchangeable ensemble representing a discrete distribution of effect trajectories. We may then obtain a sample of effect trajectories by sampling with replacement from this ensemble with all 15 ensemble members considered equally probable. Alternatively, we consider our best estimate to be the median change indicated in red in Figure 2.

3.2. Damage Cost Distribution for Baseline Sea Level

We assume that annual damage costs are independent between years. We estimate a distribution F_b for annual damage costs associated with baseline sea level based on observed damage data. Applying the relation in equation (3) to a random variable drawn from F_b then yields a random variable from the distribution

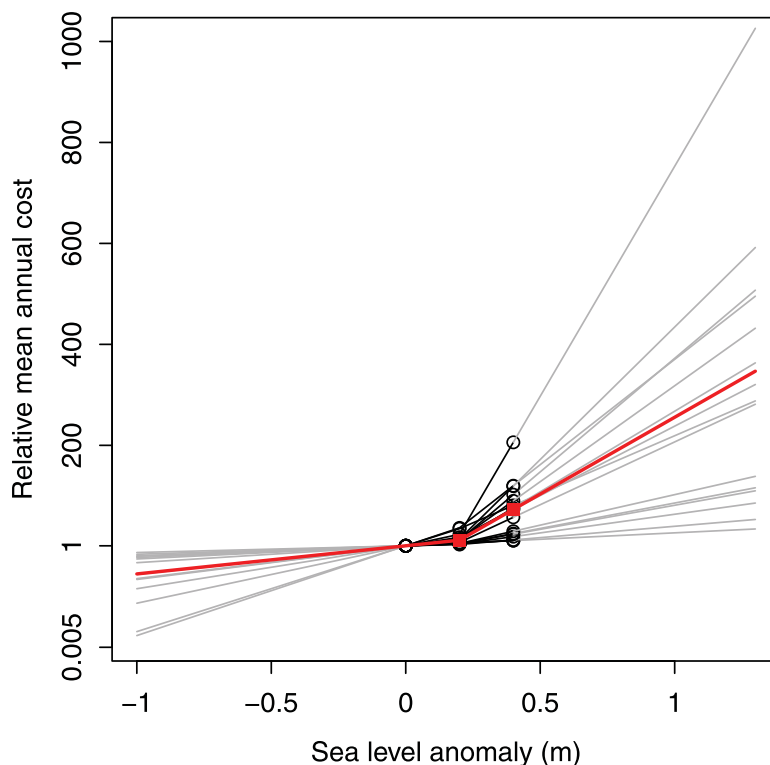


Figure 2. Relative change in mean annual damage as a function of sea level rise for 15 European cites as estimated by Hallegatte et al. [2013] (black circles) with linearly extrapolated values indicated by gray lines. The median change and the corresponding extrapolation are indicated in red.

of annual damage costs under the sea level anomaly s . Specifically, we model F_b by the three parameter Burr distribution [Burr, 1942] with two shape parameters $\alpha, \zeta > 0$ and a scale parameter $\theta > 0$. It has support on the positive real axis and its density function f_b is given by

$$f_b(x) = \frac{\alpha \zeta (x/\theta)^\zeta}{x [1 + (x/\theta)^\zeta]^{x+1}}, \tag{4}$$

for $x > 0$. The Burr distribution has a heavy upper tail and is commonly used to model damage loss [see, e.g., Klugman et al., 2012].

The parameters of the distribution are estimated using historical data for annual storm surge damage. We use 2015 cost level as our cost baseline; data prior to 2015 are adjusted to the 2015 level using the consumer price index. Assume that N such historical damage cost observations, d_1^h, \dots, d_N^h , are available. Using the corresponding historical sea level anomalies, s_1^h, \dots, s_N^h , these are then transformed to damage cost observations associated with baseline sea level using the relation in equation (3). That is, we set

$$d_n^{hb} = \frac{d_n^h}{g(s_n^h | \beta)}, \quad n = 1, \dots, N, \tag{5}$$

where g is here given by the median effect trajectory indicated with a red line in Figure 2. Finally, we estimate the parameters of the Burr distribution using the transformed data $d_1^{hb}, \dots, d_N^{hb}$.

3.3. Projected Cost Distribution

We are now interested in obtaining a probabilistic projection of present value damage costs for any year in the period 2016–2100. We include the uncertainty in (a) the sea level rise projections as described in section 2, (b) the effect of the sea level rise on damage costs as described in section 3.1, and (c) the annual damage costs as described in section 3.2. Under no adaptation, we obtain this by repeating the following four steps $J = 10,000$ times:

1. Sample a trajectory of projected sea level rise anomalies s_1, \dots, s_{85} using the methodology in section 2.
2. Sample 85 i.i.d. baseline damage cost values d_{b1}, \dots, d_{b85} from F_b .
3. Sample an effect function g from the ensemble shown in Figure 2.
4. Use the relation in equation (3) to obtain projected damage costs d_1, \dots, d_{85} .

For each year t_i where $i \in \{1, \dots, 85\}$, we then have a sample $d_i^{(1)}, \dots, d_i^{(J)}$ of J damage cost values and we define the probabilistic projection as the empirical distribution of these,

$$F_i(x) = \frac{1}{J} \sum_{j=1}^J \mathbb{1}\{d_i^{(j)} \leq x\}. \tag{6}$$

We may exclude the uncertainty in any of the three first steps by using median values rather than a random sample. Also, for comparison, we calculate the corresponding projected damage cost distribution under no sea level rise by using sea level rise anomalies for 2016 for every year 2016–2100. Alternatively, we obtain a projection of the total damage costs over the period 2016–2100 by considering the empirical distribution of the variables

$$d_{\text{total}}^{(j)} = \sum_{i=1}^{85} d_i^{(j)}, \quad j=1, \dots, J, \tag{7}$$

and similar for cumulative damage costs.

When an adaptation measure is implemented in year t_k to protect against K meters of increased sea level, the projected cost distribution changes in two ways. First, the present value adaptation cost,

$$C_k = \frac{C}{\prod_{l \leq k} (1+r_{t_l})}, \tag{8}$$

where C is the 2015 level adaptation cost, needs to be added to the damage cost in year t_k . Second, we must account for the additional K meters of protection from year t_k onward. We do this by subtracting K from the projected sea level anomaly s_i for all $i \geq k$. This assumes that the adaptation measure will provide protection from its implementation year until the end of the study period. That is, the four sampling and calculation steps above are replaced by the following four steps.

1. Sample a trajectory of projected sea level rise anomalies s_1, \dots, s_{85} using the methodology in section 2. For $i \geq k$, replace s_i by $s_i - K$.
2. Sample 85 i.i.d. baseline damage cost values d_{b1}, \dots, d_{b85} from F_b .
3. Sample an effect function g from the ensemble shown in Figure 2.
4. Use the relation in equation (3) to obtain projected damage costs d_1, \dots, d_{85} . For the implementation year k , replace d_k by $d_k + C_k$ with the adaptation cost C_k given in equation (8).

We then build the projected cost distribution in equation (6) as above.

3.4. Limitations of the Decision Framework

We consider the main limitation of this light touch decision framework the significantly simplified assessment of the effect of sea level rise on the damage costs. Within the range of sea level rise considered here, we expect the effect function to be monotonically increasing for most coastal cities in Europe. However, the linear extrapolation of the results reported in Hallegatte *et al.* [2013] for 0.2 and 0.4 m sea level rise to larger values might provide a conservative estimate of the effect of extreme sea level rise as the oreography of many cities is such that the flooded area per unit of sea level rise increases at a super-linear rate. However, with only two data points at 0.2 and 0.4 m, extrapolation approaches such as a power law or exponential growth to estimate the values for sea level rise above 1 m seem difficult to justify.

Alternatively, a modeling framework similar to that of Hallegatte *et al.* [2013] could be applied directly to a larger range of potential changes in sea level. The elements of such a framework might include an appropriate social discount rate, valuing environmental goods in monetary terms, incorporate socioeconomic assumptions, and long-term policy goals of decision-makers, as well as that climate change is often not the only driver that decision-makers should consider, therefore costs and benefits should be studied in a wider

context [Dittrich et al., 2016]. Such a model is also required for a precise estimation of the effect of an adaptation measure.

Our framework simplifies the cost and effect of an adaptation option during construction in that we assume no effect until the construction is finished with all the construction cost falling in the last year of the construction. Especially for larger constructions, these assumptions might need to be modified. Additionally, we have not specifically accounted for potential changes in storm surge patterns. Other modeling choices, such as the choice of a damage cost distribution model and discount rate are also likely to affect the results.

4. Risk Mapping

The initial scoping of climate adaptation in Esbjerg [Esbjerg Municipality, 2014] has been informed by a limited set of floods maps representing different scenarios corresponding, respectively, to flooding caused by storm surges, heavy rainfall and rising ground water levels. The flood maps themselves are produced using simplified modeling approaches representing present day climate conditions, i.e., they do not consider the expected changes in, e.g., sea level rise and rainfall characteristics caused by climate change. They also do not include an explicit representation of the urban drainage system. Thus, in the context of making decisions on adaptation this preliminary mapping is primarily meant as a tool for identifying high-risk areas, e.g., in terms of avoiding future urban development into such areas, and as a precursor for much more detailed (and resource intensive) local hydrological and economical modeling efforts, e.g., to pave the way for deciding upon cost-effective adaptation measures in the second phase of the plan. As a result, what is of relevance to the stakeholders at this stage is not the mapping of hydrological hazards by itself, but rather the mapping of risk, which compounds hazard with (economic) valuation of its consequences for any given map area or pixel. In general, this may be expressed as the probability, e.g., of a certain flood depth, derived from the urban flood model times a damage function associating the flood depth with the chosen measure of cost [e.g., Halsnæs et al., 2015]. The damage function—as in the case of Bergen—is often expressed in economic terms, however, in Esbjerg a categorical approach has been preferred, wherein a value between 1 and 10 is allocated to each map object (cf. Table 1).

Correspondingly, risk is mapped categorically on a scale from 1 to 10, where 10 indicates the highest risk level. What we observe is that buildings and critical infrastructure within this simplistic decision framework are always associated with a high risk of economic losses, whereas all other objects are in practice given a lower priority. As a result distinguishing specific high-risk areas in the built environment becomes crucially dependent on the results of the hazard modeling, which again means that considering the uncertainties can play a large role in what areas are identified.

In the following we will expand on the existing light touch approach used in Esbjerg to identify areas susceptible to coastal floods, to test the importance of considering uncertainties related to projections of sea level rise and storm surges, as well as uncertainties related to the probability of occurrence. The latter will be done by comparing the consequences of storm surge events of different severity: a moderately likely 20 years and an extreme 100 years return event (return periods calculated from historical storm surge statistics).

Table 1. Categorical Risk Values Allocated to Delimited Map Areas in Esbjerg on a Squared Grid, Prescribed by the End-Users^a

Map Object	Description	Value
Important buildings	E.g., industry, hospitals and other public buildings	10
Other buildings	All other building types than the above	8
Critical infrastructure	Waste water treatment plant, railroads, etc.	10
Roads	Essentially all types of roads from main roads to minor paths	6
Cultural heritage	Including cemeteries, historical landscape	0.1–4
Natural systems	Included protected areas and sports facilities	0.1

^aA value of 10 indicates the highest risk of economic losses associated with flooding, whereas 0 indicates an inconsequential risk. The value allocated to specific grid squares correspond to a weighted average of the map objects within, e.g., buildings and infrastructure.

5. Case Studies

5.1. Background

The Norwegian city of Bergen is the capital of Hordaland County. The city center is located on Byfjorden and is surrounded by mountains. It has the largest port in Norway, both in terms of freight and passengers. The historic harbor area, Bryggen, is the only Hanseatic trade center remaining in its original style,

and has been declared a UNESCO World Heritage site (see <http://whc.unesco.org/en/list/59>). Bryggen is regularly flooded at extreme tides, and it is feared that as sea levels rise, floods will become a major problem in other parts of Bergen as well [Grieg Foundation, 2009]. This report does a very rough projection of sea level rise and storm surges in Bergen, applying their 90% estimate of highest flooding to a digital terrain map of Bergen to determine where the main problems are located.

The municipality of Bergen has, in cooperation with private actors, analyzed several possible adaptation measures against sea level rise. The measures range from an outer barrier that would protect the entire metropolitan area to various protection measures of limited areas in the inner harbor [Grieg Foundation, 2009]. While the viability of the constructions and the associated construction costs have been carefully analyzed, the optimal timing of potential adaptation measures and the effects of the associated uncertainties have yet to be investigated. We perform such an analysis where we consider uncertainty in projected sea level rise, damage costs, and the effect of sea level rise on changes in damage costs.

Esbjerg, on the southwest coast of Jutland, is the fifth-largest city in Denmark and the largest urban area in the region. The city hosts one of the largest harbors in Denmark, which serves as a focal point for offshore activities in the North Sea, including the continued development of offshore wind power and extensive activities related to the extraction of oil and gas. As a result, critical infrastructures and commercial buildings figure prominently in the coastal zone. Esbjerg is frequently subject to substantial storms and storm surges, causing severe flooding of the harbor and the city. The highest since records began in 1874 was recorded in 1981, where the harbor was completely flooded and the water level reached 4.33 m above the norm, causing massive economic losses. More generally, storm surges causing water levels in Esbjerg to rise to between 2 and 3 m have quadrupled over the last four decades according to local records, whereas half of the most severe events have taken place since 1975.

As in the case of Bergen, sea level rise caused by climate change is expected to compound these risks, alongside parallel threats caused by increased risks of pluvial flooding and rising ground water levels in Esbjerg. On this background and prompted by national legislation the local government of Esbjerg recently adopted a framework, which defines two phases of climate adaptation in the municipality for the period of 2014–2026.

In the first phase of the plan, the principal aim for the municipality is to identify present and future flood-prone areas, e.g., to avoid urban development in such areas and to limit damages to buildings of high societal or cultural value. The decision-problem as formulated by the local government itself is “to not allow urban development into an area unless it is probable that the location is not flood-prone or if the flood risk can be mitigated appropriately” [Esbjerg Municipality, 2014]. Following this line of reasoning an initial set of risk and value maps were commissioned from a Danish consultancy company, i.e., to form the basis for identifying specific areas or locations within the municipality for more detailed investigation and hydrological modeling during the second phase (see section 4). Interestingly, the municipality currently considers pluvial floods to be the more urgent focus. However, on the long term the risk of coastal flooding is expected to dominate (with groundwater posing as an unknown), suggesting that new management and decision-making alternatives may be required at a potential future “cross-over point” [Guillaume *et al.*, 2016]. Actionable methods for analyzing decision-problems in the presence of cross-over points have been developed, e.g., by Guillaume *et al.* [2016], but since the present case study only considers the first phase of the Esbjerg climate adaptation plan, they were not applied.

As already mentioned, assets in Esbjerg that are susceptible to flooding are ranked using a simple categorical approach, omitting any detailed and site-specific economic analysis. Hence at this point the municipality is evidently neither taking into account physical nor economic uncertainties. Interactions with the local authorities also did not reveal at what level this will be addressed in the next stages of the risk assessment. Conversely, the authorities were very much aware of the shortcomings of the initial analysis, and improved information in this regard was found to be in high demand. In the following we expand on the initial analysis of the flood risk, considering both the uncertainty in projected sea level rise and the potential implications related to the risk assessment.

5.2. Data

The historical global mean temperature series is obtained from Hansen *et al.* [2001]. Climate projections of global mean temperature are from the fifth climate model intercomparison project, CMIP5 [Taylor *et al.*,

2012]. The global mean sea level series is obtained from Church and White [2011]. We use local tide gauge data from the Permanent Service for Mean Sea Level, UK, which is the worldwide repository for national sea level data. Glacial isostatic adjustment for Bergen is obtained from Simpson *et al.* [2014], and for Esbjerg in personal communication from Peter Thejll at the Danish Meteorological Institute.

The Bergen monthly series is missing data for 62 months, including all of the years 1942–1943. To deal with occasional short stretches of missing data (at most one or two months), we use median polish replacement [Mosteller and Tukey, 1977], a robust two-way additive fit, and then compute annual averages. For the years 1942–1943, we use the average difference between Bergen and the average of all other Norwegian stations in 1940 and 1943 to estimate values for 1941 and 1942, using the average of all other Norwegian stations corrected by the average difference.

The Esbjerg monthly series is missing data for 19 months. Here, too, we use median polish to fill in missing data and then compute annual averages.

Annual damage costs for the Bergen case study are obtained from the Norwegian Natural Perils Pool (NPP) at <https://www.finansnorge.no/statistikk/skadeforsikring/Naturskadestatistikk-NASK/>. The NPP data are available for the period 1980–2015 and are aggregated to a county level. For improved parameter estimation, we include the data from Rogaland county which is the county directly south of Hordaland and with similar characteristics. We use a discount rate of 4% for the first 40 years of the analysis, a rate of 3% for 40 to 75 years into the future and a rate of 2% beyond 75 years [cf. Norwegian Ministry of Finance, 2012, section 5.8].

Storm surge data for Esbjerg are obtained from the Danish Coastal Authority [Sorensen *et al.*, 2013].

5.3. Sea Level Rise in Bergen and Esbjerg

Figure 3 shows uncorrected and corrected Bergen sea level data, and the relationship between the corrected Bergen data and the global sea level data (see equation (2)). The glacial isostatic adjustment is 0.0026 (standard error 0.0007) m/yr. The time series regression uses an ARMA(1,1)-model [Box and Jenkins, 1970], with AR parameter 0.82 (0.13), and MA parameter -0.61 (0.17). The regression slope is 1.30 (0.12).

For the relationship between global annual mean temperature and global annual mean sea level rise we use the results from Bolin *et al.* [2014]. Figure 4 (left) shows the simultaneous 90% confidence region for Bergen sea level rise relative to 1999 under scenario RCP 8.5, which is the scenario Norwegian authorities recommend for planning purposes.

For Esbjerg, the glacial isostatic adjustment is 0.0006 (0.0003) m/yr. The time series regression model (2) relating gia-corrected local to global sea level is an MA(1) model with parameter 0.17 (0.09). The regression

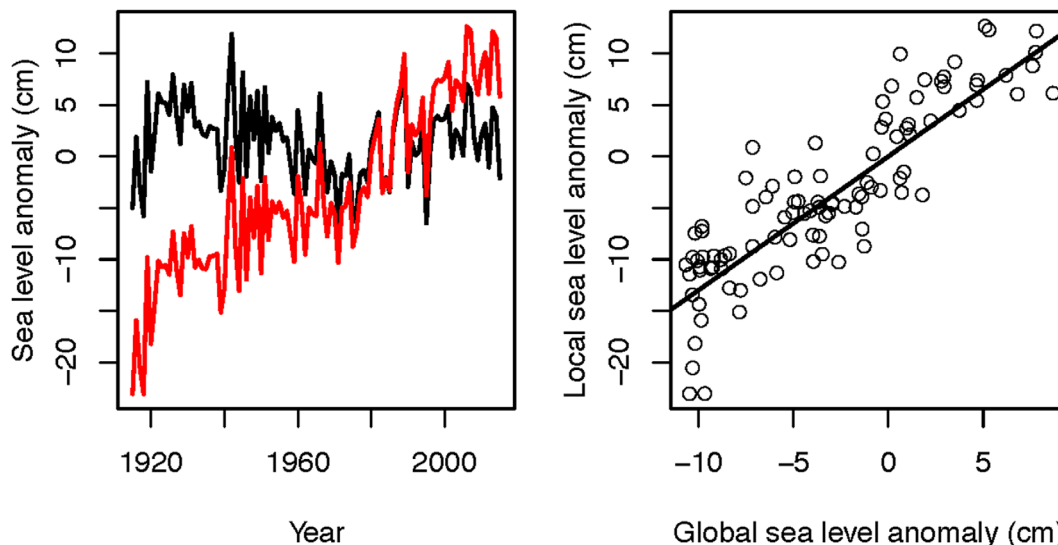


Figure 3. The left figure shows raw (black) and gia-corrected (red) sea level data from Bergen. The right figure relates the gia-corrected Bergen sea level to the global sea level series of Church and White [2011]. The straight line is the time series regression line.

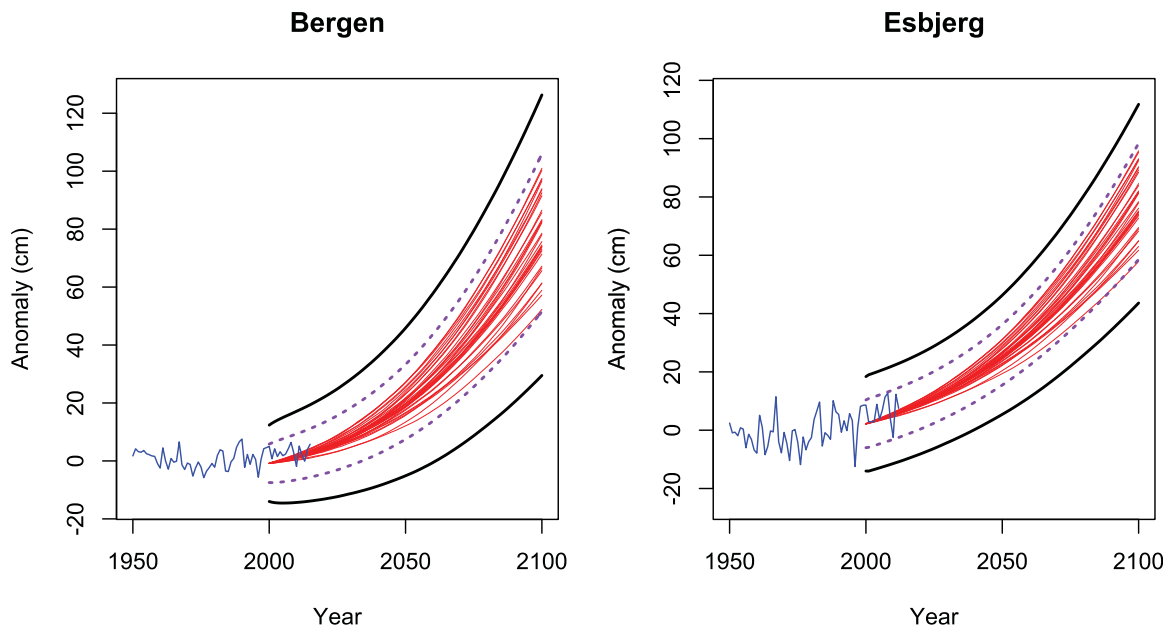


Figure 4. Simultaneous 90% confidence set (thick black lines) for Bergen (left) and Esbjerg (right) sea level projections for the years 2000–2100 using RCP 8.5. The sea level data for 1950–2015 are shown in blue. The thin red lines are the projections without uncertainty based on each of the climate models. The dashed purple lines connect pointwise confidence intervals for each year.

slope is 1.02 (0.06). Figure 4 (right) shows the simultaneous 90% confidence region for sea level rise relative to 1999 under scenario RCP 8.5.

5.4. Timing of Adaptation Measures in Bergen

Figure 5 shows the histogram of observed annual damage costs for Bergen and the associated Burr distribution. The parameter estimates are $\hat{\alpha}=3.94$, $\hat{\gamma}=0.48$, and $\hat{\theta}=0.26$. *Grieg Foundation* [2009] discuss several different adaptation options for Bergen. In Figure 6 we consider the optimal timing of an adaptation option that includes two inner barriers at Vågen and Damgårdssundet, that is, one on each side of central Bergen. The combined construction cost of the two barriers for a protection against 0.75 m sea level rise is estimated at 1.13 billion Norwegian Kroner (NOK) at the 2015 level (100 NOK is about 11 EUR or 12 USD). As

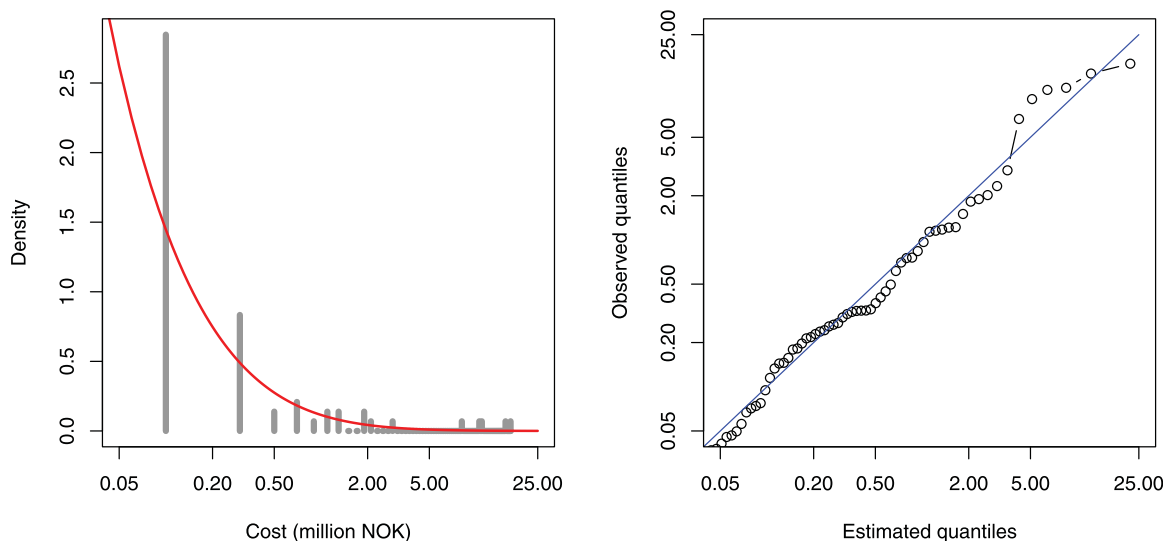


Figure 5. (left) Estimated density function of annual damage costs in Bergen for 2015 (red) based on observed annual damage in Hordaland and Rogaland counties 1980–2015 (gray bars). (right) Q-Q plot comparing empirical and estimated quantiles with the line $x = y$ indicated in blue.

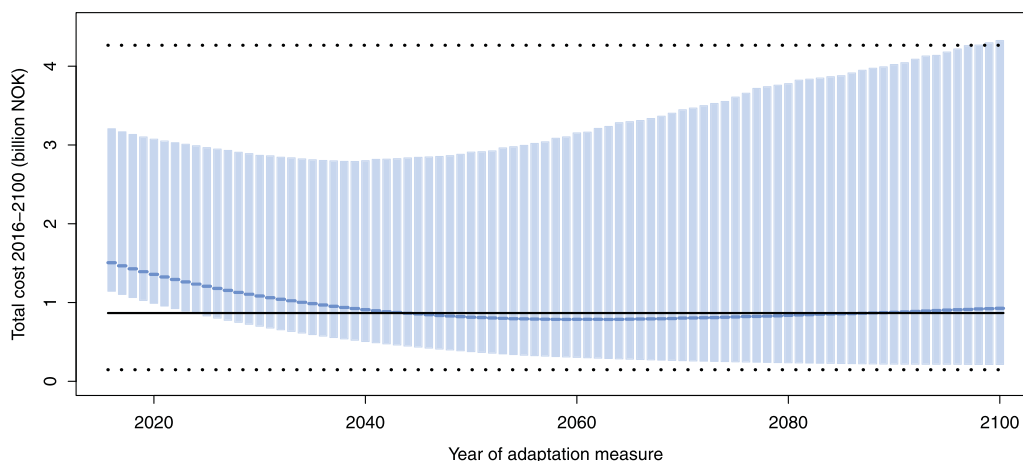


Figure 6. Projected aggregated damage costs in Bergen over the time period 2016–2100 as a function of the timing of an adaptation measure consisting of the construction of two inner barriers. The median projection under each adaptation scenario is indicated in blue with light blue bars denoting the 90% projection intervals. The median projected total damage cost under no action is shown with a black line with the corresponding 90% projection interval indicated by dotted lines.

the inner barriers only provide partial areal protection, we assume that they have a mitigating effect on 50% of damages incurred by storm surges.

In an analysis that combines sea level projections and terrain information for Bergen, *Grieg Foundation* [2009] conclude that adaptation measures need not be implemented before 2065. This analysis did not include specific projections of damage cost. Applying the methodology from section 3 we find that according to our median projection, the optimal time of building the barriers is around the same time, in 2059 (Figure 6). Compared to no adaptation, an adaptation measure completed in 2059 will on average save about 9% of the median damage costs by the year 2100, where a significant part of the total projected cost under adaptation is due to the adaptation construction cost (Figure 7). At the high end (or the 95th percentile of the damage distribution), the optimal adaptation time is over a quarter of a century earlier in 2039. An adaptation measure implemented at this time will save about 35% when the 95th percentiles of the distributions are compared while we expect to save about 27% at this percentile for an adaptation measure implemented in 2059.

Furthermore, *Grieg Foundation* [2009] consider a far-reaching protection measure consisting of an outer barrier that would protect the whole metropolitan area. The cost of this construction is estimated to be at least 34 billion NOK (2015 level). It is assessed that such a construction is not viable due to large environmental and economic consequences. Our estimates of the total damage (Figure 7) support this conclusion.

5.5. Identifying Flood-Prone Areas in Esbjerg

Table 2 contains the total projected storm surges for Esbjerg, corresponding to 20 year and 100 year historical surges, with and without considering the projected sea level rise. The first column shows the historical storm surge statistics based on 139 years of observations in Esbjerg Harbor [Sorensen *et al.*, 2013], where the numbers in brackets indicate the standard deviation derived from a statistical analysis. The following columns indicate future storm surge water levels, constructed by adding the projected sea level rise corresponding to the 10th percentile, median, and 90th percentile of the distribution shown in Figure 4 to the values inferred historical storm surge statistics. We therefore implicitly assume that, e.g., the statistics of a 20 years return event will remain unchanged in the projection period. We see that using our projections the historical maximum of 4.33 m is almost certain to be exceeded by 2100.

Figure 8 shows flood maps for Esbjerg corresponding to the entries in Table 2, based on data provided by the Danish Geodata Agency (see <http://download.kortforsyningen.dk/content/havstigning-410-500-cm>). The figure indicates the expected flood depth, derived using a simple hydrologically adapted topographical model. More information on this model are available at <http://www.klimatilpasning.dk/kommuner/kortlaegning-til-brug-for-klimatilpasning/den-kommunale-risikokortlaegning/kyst.aspx> (in Danish). These maps

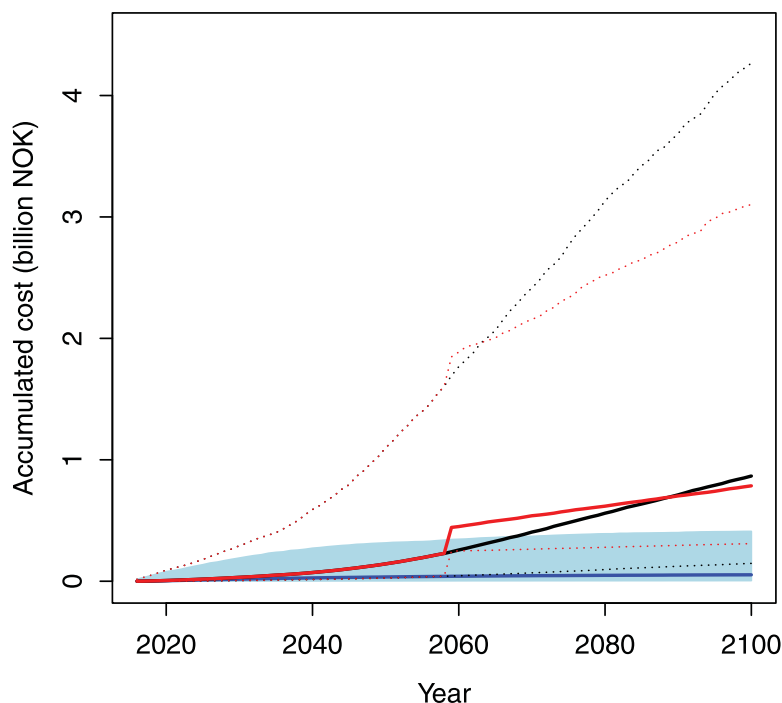


Figure 7. Median projected cumulative damage costs in Bergen under constant sea level (blue line), under sea level rise according to RCP 8.5 with no adaptation action (black line) and with the construction of two inner barriers in 2059 (red line). The shaded light blue area denotes the 90% projection interval under constant sea level. Dotted lines indicate the 90% projection intervals with sea level rise according to RCP 8.5.

are similar to the maps employed in the first phase of the Esbjerg climate adaptation plan. The blue and red color scales show the results for the 20 and 100 years return events, whereas the frames left through right corresponds, respectively, to (a) no sea level rise/present day conditions (b) 10th percentile of the sea level rise distribution, (c) the median and (d) the 90th percentile.

The most remarkable feature in Figure 8 is the apparent dike breach, which results in massive flooding to the northwest of Esbjerg, when considering the 90th percentile both for 20 and 100 years return events, and which does not appear when considering only the median. Second, it is also clear that the differences between 20 and 100 years return storm surge events both in terms of the areas flooded and the flood depth overall are found to be relatively small, implying that already a moderate storm surge may potentially have high impacts. When further accounting for the projected sea level rise as shown in Figure 4 such events are likely to appear considerably more frequent in the future.

Lastly, in terms of the harbor and the coastal areas which are dominated by high-value objects such as critical infrastructure, industry, and buildings a clear relation between the flood depth and the severity of the storm surge is observed. This suggests that to properly identify the risk and thus pave the way for deciding upon cost-effective adaptation measures, it is crucial to consider not only the median but the full range of hydrological projections.

6. The Value of Including Uncertainty

6.1. Sea Level Projections

In many cases sea level rise projections are given as a single number for each scenario, usually the mean or median of the ensemble of projections from different climate models [e.g., Mote et al., 2008]. Sometimes the spread of the ensemble is

Table 2. Storm Surge Water Levels [Sorensen et al., 2013] With a Return Period of 20 Years (RP20) and 100 Years (RP100) With No Sea Level Rise and With Sea Level Rise Corresponding to RCP 8.5 (10th Percentile, Median, and 90th Percentile)

Storm Surge	No Sea Level Rise	RCP 8.5		
		10th Percentile	Median	90th Percentile
RP20	3.62 (±0.11) m	4.31 m	4.64 m	5.00 m
RP100	4.05 (±0.16) m	4.48 m	4.81 m	5.17 m

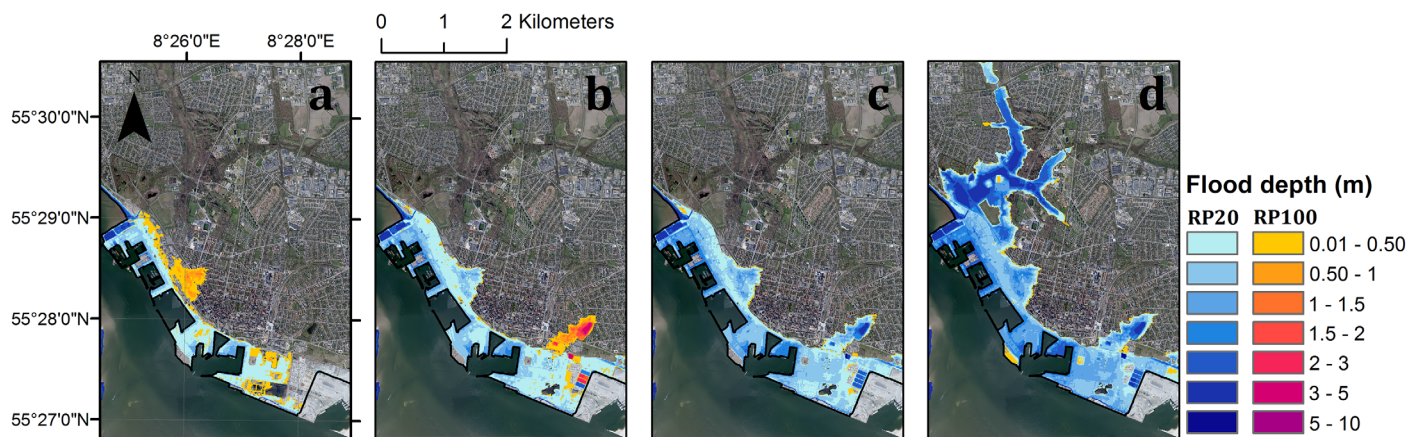


Figure 8. Flood extents and depths for the city of Esbjerg in year 2100 during storm surges with a return period of 20 years (RP20) and 100 years (RP100) with (a) no sea level rise and with sea level rise corresponding to RCP 85 (10th percentile (b), median (c), and 90th percentile (d)).

used to assess the uncertainty in the projections (e.g., the Norwegian Environmental Agency recommends using the upper ensemble value for RCP 8.5 as the basis for planning decision, pers. comm. from Even Nilsson, Norwegian Mapping Authority). In our analysis, there are two more sources of uncertainty, namely the two regression models (1) and (2). Figure 9 shows the single number (vertical black line), the ensemble spread (histogram), the uncertainty including only the global model (red) and the full uncertainty (blue) for Bergen and Esbjerg projections of sea level rise relative to 1999 under RCP 8.5. For Bergen, we see that the ensemble 90% range is 0.12 m, whereas the overall 90% confidence range is about 0.24 m. While the values for Esbjerg are somewhat higher, there is slightly less uncertainty in the projections.

6.2. Damage Costs

A simplistic analysis of projected total damage costs for the year 2100, not taking into account the uncertainty, would use the median historical damage cost multiplied by the median damage effect factor at 2100 at the median sea level rise projected for 2100. Performing this exercise for every year 2016–2100 yields a

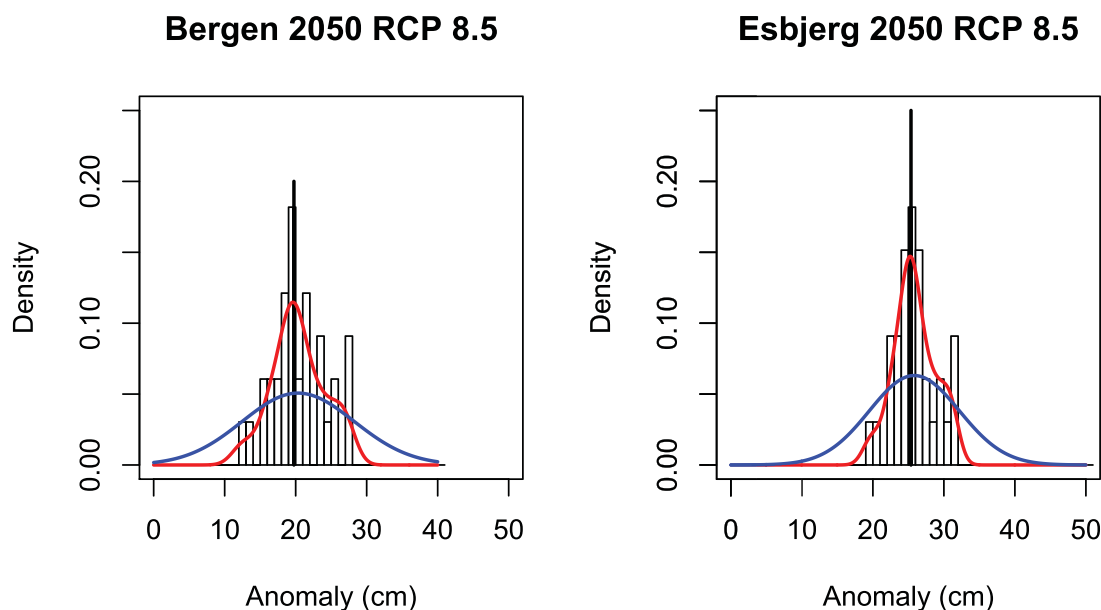


Figure 9. 2050 Bergen (left) and Esbjerg (right) sea level projections with uncertainty due to different sources for RCP 8.5. The black vertical line is the median projection (with no uncertainty), while the gray histogram corresponds to the spread of the climate models, the red curve adds the uncertainty due to the relation between global temperature and global sea level, and the blue line that due to downscaling global sea level to Bergen.

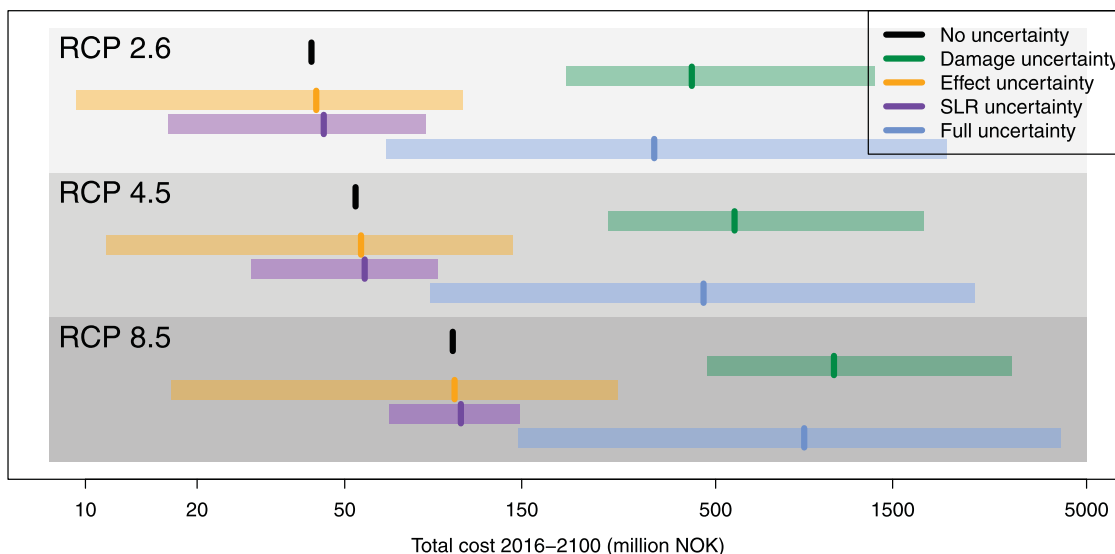


Figure 10. Median estimates and 90% intervals of total accumulated damage cost for 2016–2100 without adaptation for five different uncertainty assumptions and three different sea level rise scenarios (RCP 2.6, 4.5, and 8.5). Estimates using medians of all components are shown in black and results accounting for all aspects of uncertainty are shown in blue. We also show the distributions of costs varying only one aspect of the uncertainty (sea level rise in purple, effect multiplier in yellow, and damage cost in green), holding the other two at their median values.

total (discounted) damage cost of 98 million NOK under the RCP 8.5 scenario used in section 5.4 (the black vertical line in the bottom third of Figure 10). Similar results are obtained when allowing sea level or effect factor to vary, holding the other quantities at the median (yellow and purple vertical lines in the bottom third of Figure 10). However, allowing only the damage cost to vary yields a median total cost of 1042 million (green vertical line in the bottom third of Figure 10). The appropriate uncertainty analysis for our model should draw each of sea level, effect factor and damage cost at random from their distributions for 2016–2100. This corresponds to a total median cost of 866 million NOK, approximately 9 times higher than the simplistic value (blue vertical line in the bottom third of Figure 10). Over 99% of the costs in our simulation are higher than the simplistic median.

Using scenarios RCP 2.6 and RCP 4.5 rather than RCP 8.5 results in overall lower total damage values (the two upper panels of Figure 10). Accounting for all three uncertainty aspects yields a median total damage of 456 million NOK under RCP 4.5 and 351 million NOK under RCP 2.6. However, the relative effect of including uncertainty remains the same: The median total damage under the full uncertainty analysis is roughly 9 times larger than the analysis that does not account for uncertainty for all three RCP scenarios. Note also that even if the estimates are somewhat lower for the less conservative RCP scenarios, there is a large overlap between the resulting distributions. Under RCP 2.6 and full uncertainty analysis, we estimate that there is a 21% probability of the cost being larger than the median estimate of 866 million NOK under RCP 8.5. Under RCP 4.5, the probability of exceeding this number is 28%. Note that the width of the 90% interval is roughly the same for all three RCP scenarios when only the uncertainty in the sea level projections is accounted for. For all the other cases, the width of the 90% interval under RCP 8.5 is more than twice that under RCP 2.6.

6.3. Risk Assessment

The simple spatial analysis carried out for Esbjerg as a screening tool for identifying high-risk areas considers not only the median result but also higher and lower order percentiles as well as different storm surge intensities. Such a probabilistic approach is clearly needed in order to correctly identify areas susceptible to a high risk of flooding, which may subsequently be the subject of more detailed hydrological modeling related, e.g., to the potential design and implementation of concrete adaptation measures.

Seen from the perspective of a decision-maker, however, adaptation actions are likely to be related to an assessment of risk and not hazard. Figure 11 illustrates such a risk assessment and depicts the situation with (right), respectively, without (left) uncertainty information included. In both cases the risk of flood

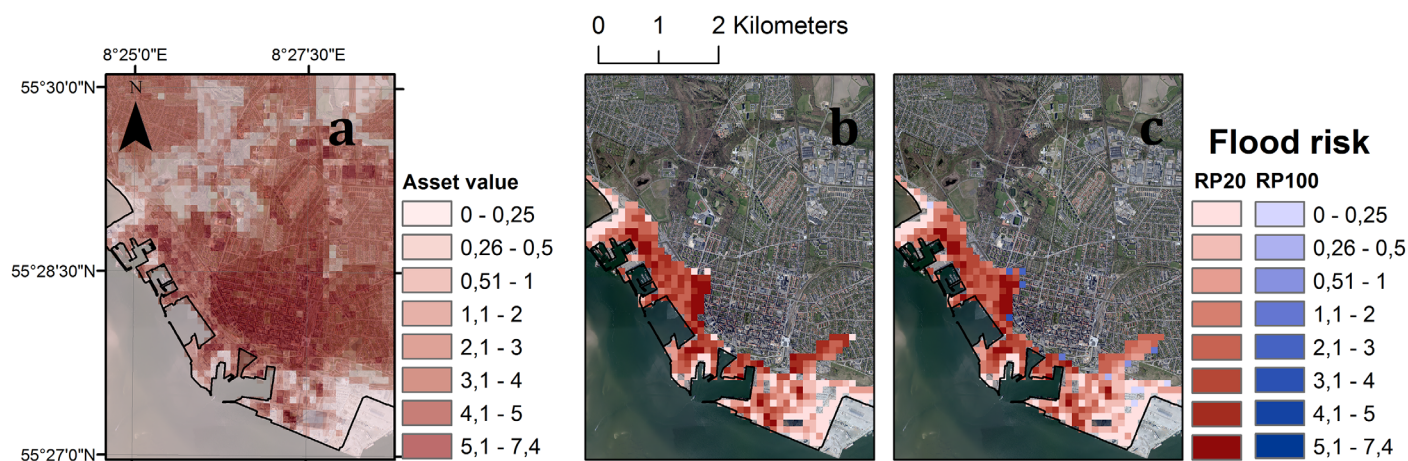


Figure 11. (a) User valuation of assets in Esbjerg (cf. Table 1). The value assigned to any given pixel is equal to the sum of co-located map objects. (b) Risk of a flood exceeding 0.1 m for a 20 years return event, similar to the mapping carried out by the municipality [Esbjerg Municipality, 2014]. Unlike the impact assessment used for first phase of the Esbjerg climate adaptation plan, sea level rise under the RCP 8.5 scenario is here considered, corresponding to the median projection. No further moments are considered. (right) Risk of a flood exceeding 0.1 m for a 20 and 100 years return events, respectively. For each pixel the probability for the flood level to exceed 0.1 m is estimated based on projections of the 10th, median, and 90th percentile.

levels exceeding 0.1 m is shown. The left panel presents the situation as faced by the municipal decision-maker after the initial risk mapping. Pixels where the flood level exceeds 0.1 m during a 20 years return event have a probability of one, and hence the risk level is given primarily by the valuation of assets. For comparison, the right panel shows the result of our light touch analysis, considering uncertainties related to the spread of the climate model ensemble and the intensity of the storm surge. The pixel-wise probabilities are calculated based on the sea level projections, e.g., the severity of the events (20 years versus 100 years return values) and the spread of the ensemble (represented by projections corresponding to the 10th and 90th percentile). Making the simplifying assumption that for each pixel the uncertainty follows a Gaussian distribution, we calculate the mean and spread for each pixel, and based on this infer the probability of flood levels exceeding 0.1 m from the associated cumulative distribution function. This assumption evidently does not hold in all cases but provides a fast and efficient way to assess the probability based on only a few projections and was found to yield reasonably accurate estimates.

From Figure 11 we find that for some areas (c) the risk is reduced when considering the estimated uncertainty as compared to the case where uncertainties are not considered (b). Given the overall decision-problem stated by Esbjerg's climate adaptation plan this suggests that ignoring the uncertainties can lead to a poor identification of the flood-prone areas both in terms of underestimating and overestimating the risk. Interestingly, the impact of a 100 years storm surge is found to be only marginally different than that of a 20 years event, indicating that implementing suitable adaptation measures are likely to yield a high level of security. Admittedly, this result is severely compounded by the simplistic categorical valuation scheme used for the risk assessment (a). Hence by design this scheme does not discriminate sufficiently between assets to allow for an objective prioritization based on the underlying data, i.e., all buildings are generally assigned a high value compared to other assets, whereas uncertainties related to the valuation model are ignored. Rather also the uncertainties introduced by the valuation model should be introduced into the probabilistic modeling chain, since the underlying economic assumptions and modeling [Halsnæs et al., 2015] can have significant implications on the final results of the risk mapping. One example of this, as already highlighted in the current scheme (Table 1), is the valuation of natural areas, which in the context of the Esbjerg case in particularly relates to the marshes close to the nearby city of Ribe that are protected under the code of Natura 2000 (see http://ec.europa.eu/environment/nature/natura2000/index_en.htm). From stakeholder interviews, it is evident that assigning an objective value to this area, whether by economic cost or in terms of a score, which aligns with the overall objectives of the adaptation plan is a difficult task, which must be taken into account when making the risk assessment including a quantification of the uncertainties from the end-users' perspectives.

7. Conclusions

Sea level rise has serious consequences for infrastructure in coastal areas. Our case studies demonstrate that it is possible to take uncertainty into account in deciding when and where to implement adaptation measures, even if one uses light touch decision-making approaches. Failing to account for uncertainty can result in bad scenarios, such as 95th percentiles, to be an order of magnitude worse than what the planners are expecting. For climate change adaptation in general, it is likely worthwhile to be pessimistic in the planning and in the projections in accordance with the precautionary principle. As an example, the Norwegian Government recommends all assessments of the impacts of climate change to be based on figures from the high end of the range of national climate projections [Norwegian Ministry of Climate and Environment, 2013].

We consider our case studies proofs of concept and see these as first steps in a sequence of interactions with local planners and other end-users. The adaptation planning process has to be an iterative and interactive process, as the decision framework provides actionable information to decision-makers, who will then make their own decisions. These decisions can then be incorporated into the current adaptation strategy. Further simulation studies allow a continued loop to identify potential vulnerabilities of the approaches across a wide range of possible futures.

Down the line we plan to develop a flexible and easy-to-use tool kit for decision-making under uncertainty regarding sea level rise. An initial step in this direction is the software used in this analysis, which is publicly available and uses free software.

Acknowledgments

This work was funded by NordForsk through project number 74456 "Statistical Analysis of Climate Projections" (eSACP) and The Research Council of Norway through project number 243953 "Physical and Statistical Analysis of Climate Extremes in Large Datasets" (ClimateXL). The authors thank four anonymous reviewers for thoughtful, constructive comments which substantially improved the paper. The source code for the analysis is implemented in the statistical programming language R [R Core Team, 2016] and is available on GitHub at <http://github.com/eSACP/SeaLevelDecisions/Code> together with the local sea level projection data and the damage cost data for Bergen.

References

- Bamber, J., and W. Aspinall (2013), An expert judgement assessment of future sea level rise from the ice sheets, *Nat. Clim. Change*, 3, 424–427.
- Bisaro, A., R. Swart, and J. Hinkel (2016), Frontiers of solution-oriented adaptation research, *Reg. Environ. Change*, 16(1), 123–136.
- Bolin, D., and F. Lindgren (2015), Excursion and contour uncertainty regions for latent gaussian models, *J. R. Stat. Soc. B*, 77(1), 85–106.
- Bolin, D., P. Guttorp, A. Januzzi, M. Novak, H. Podschwit, L. Richardson, C. Sowder, A. Särkkä, and A. Zimmerman (2014), Statistical prediction of global sea level from global temperature, *Stat. Sin.*, 25, 351–367.
- Box, G., and G. Jenkins (1970), *Time Series Analysis: Forecasting and Control*, Holden-Day, San Francisco.
- Burr, I. W. (1942), Cumulative frequency functions, *Ann. Math. Stat.*, 13(2), 215–232.
- Chambwera, M., G. Heal, C. Dubeux, S. Hallegatte, L. Leclerc, A. Markandya, B. McCarl, R. Mechler, and J. Neumann (2014), Economics of adaptation, in *Climate Change 2014: Impacts, Adaptation, and Vulnerability. Part A: Global and Sectoral Aspects. Contribution of Working Group II to the Fifth Assessment Report of the Intergovernmental Panel on Climate Change*, pp. 945–977, Cambridge University Press, New York.
- Church, J., and N. White (2011), Sea-level rise from the late 19th to the early 21st century, *Surv. Geophys.*, 32, 585–602.
- de Bruin, K., and T. L. Thorarinsdottir (2016), Report from a workshop on practical and methodological challenges of climate change adaptation, *Tech. Rep. SAMBA/32/16*, Norwegian Computing Center, Oslo. [Available at https://www.nr.no/thordis/files/Report_AdaptationWSforPractitioners.pdf]
- Dittrich, R., A. Wreford, and D. Moran (2016), A survey of decision-making approaches for climate change adaptation: Are robust methods the way forward?, *Ecol. Econ.*, 122, 79–89.
- Downing, T. E. (2012), Views of the frontiers in climate change adaptation economics, *WIREs Clim. Change*, 3(2), 161–170.
- Esbjerg Municipality (2014), *Klimatilpasningsplan for Esbjerg*, technical report, Esbjerg: Esbjerg Municipality, Denmark.
- Fankhauser, S., and R. Soare (2013), An economic approach to adaptation: Illustrations from Europe, *Clim. Change*, 118(2), 367–379.
- Fankhauser, S., J. Smith, and R. S. J. Tol (1999), Weathering climate change: Some simple rules to guide adaptation decisions, *Ecol. Econ.*, 30, 67–78.
- Grieg Foundation (2009), *Regional havstigning – prosjektrapport*, technical report, Grieg Found., Visjon Vest and GØ Rieber Fondene, Bergen.
- Groves, D. G., and R. J. Lempert (2007), A new analytic method for finding policy-relevant scenarios, *Global Environ. Change*, 17(1), 73–85.
- Guillaume, J. H., M. Arshad, A. J. Jakeman, M. Jalava, and M. Kumm (2016), Robust discrimination between uncertain management alternatives by iterative reflection on crossover point scenarios: Principles, design and implementations, *Environ. Modell. Software*, 83, 326–343.
- Guttorp, P., D. Bolin, A. Januzzi, D. Jones, M. Novak, H. Podschwit, L. Richardson, A. Särkkä, C. Sowder, and A. Zimmerman (2014), Assessing the uncertainty in projecting local mean sea level from global temperature, *J. Appl. Meteorol. Climatol.*, 53, 2163–2170.
- Hallegatte, S., A. Shah, R. Lempert, C. Brown, and S. Gill (2012), *Investment Decision Making Under Deep Uncertainty Application to Climate Change*, The World Bank, Washington, D. C.
- Hallegatte, S., C. Green, R. J. Nicholls, and J. Corfee-Morlot (2013), Future flood losses in major coastal cities, *Nat. Clim. Change*, 3(9), 802–806.
- Halsnæs, K., P. Kaspersen, and M. Drews (2015), Key drivers and economic consequences of high-end climate scenarios: Uncertainties and risks, *Clim. Res.*, 64, 85–98.
- Hansen, J., R. Rued, M. Sato, M. Imhoff, W. Lawrence, D. Easterling, T. Peterson, and T. Karl (2001), A closer look at United States and global surface temperature change, *J. Geophys. Res.*, 106, 23,947–23,963.
- Hill, M. C., D. Kavetski, M. Clark, M. Ye, M. Arabi, D. Lu, L. Foglia, and S. Mehl (2016), Practical use of computationally frugal model analysis methods, *Groundwater*, 54, 159–170.
- Hinkel, J., and A. Bisaro (2016), Methodological choices in solution-oriented adaptation research: A diagnostic framework, *Reg. Environ. Change*, 16(1), 7–20.

- Jevrejeva, S., L. P. Jackson, R. E. M. Riva, A. Grinsted, and J. C. Moore (2016), Coastal sea level rise with warming above 2°C, *Proc. Natl. Acad. Sci. U. S. A.*, *113*(47), 13342–13347, doi:10.1073/pnas.1605312113.
- Jones, R., A. Patwardhan, S. Cohen, S. Dessai, A. Lammel, R. Lempert, M. Mirza, and H. von Storch (2014), Foundations for decision making, in *Climate Change 2014: Impacts, Adaptation, and Vulnerability. Part A: Global and Sectoral Aspects. Contribution of Working Group II to the Fifth Assessment Report of the Intergovernmental Panel on Climate Change*, pp. 195–228, Cambridge Univ. Press, Cambridge, U. K.
- Klugman, S. A., H. H. Panjer, and G. E. Willmot (2012), *Loss Models: From Data to Decisions*, vol. 715, 3rd ed., John Wiley, Hoboken, N. J.
- Konikow, L. F. (2011), Contribution of global groundwater depletion since 1900 to sea level rise, *Geophys. Res. Lett.*, *38*, L17401, doi: 10.1029/2011GL048604.
- Mosteller, F., and J. W. Tukey (1977), *Data Analysis and Regression*, Addison-Wesley, Reading, Mass.
- Mote, P., A. Petersen, S. Reeder, H. Shipman, and L. W. Binder (2008), Sea level rise in the coastal waters of Washington State, technical report, 549, Univ. of Washington Clim. Impacts Group, Seattle.
- Norwegian Ministry of Climate and Environment (2013), Climate change adaptation in Norway, meld. St. 33 (2012–2013), Report to the Storting (white paper), Oslo. [Available at <https://www.regjeringen.no/en/dokumenter/meld.-st.-33-20122013/id725930/sec9>].
- Norwegian Ministry of Finance (2012), Cost-benefit analysis, *Off. Norwegian Rep. NOU 2012*, 16, Oslo.
- Rahmstorf, S. (2007), A semi-empirical approach to projecting future sea-level rise, *Science*, *315*, 368–370.
- Rahmstorf, S., M. Perrette, and M. Vermeer (2011), Testing the robustness of semi-empirical sea level projections, *Clim. Dyn.*, *39*, 861–875.
- R Core Team (2016), *R: A Language and Environment for Statistical Computing*, R Found. for Stat. Comput., Vienna.
- Simpson, M. J. R., K. Breili, and H. P. Kierulf (2014), Estimates of twenty-first century sea-level changes for Norway, *Clim. Dyn.*, *42*, 1405–1424.
- Sorensen, C., H. T. Madsen, and S. B. Knudsen (2013), *Hojvandsstatistikker 2012*, technical report, Kystdirektoratet, Lemvig, Denmark.
- Stocker, T., D. Qin, G.-K. Plattner, M. Tignor, S. K. Allen, J. Boschung, A. Nauels, Y. Xia, V. Bex, and P. Midgley (2013), *Climate Change 2013: The Physical Science Basis. Contribution of Working Group I to the Fifth Assessment Report of the Intergovernmental Panel on Climate Change*, Cambridge Univ. Press, Cambridge, U. K.
- Taylor, K., R. Stouffer, and G. Meehl (2012), An overview of CMIP5 and the experiment design, *Bull. Am. Meteorol. Soc.*, *93*, 485–498.
- Thorarinsdottir, T. L., and K. de Bruin (2016), Challenges of climate change adaptation, *Eos*, *97*, doi:10.1029/2016EO062121.
- van Vuuren, D. P., et al. (2011), The representative concentration pathways: an overview, *Clim. Change*, *109*, 5–31.
- Wada, Y., L. P. H. van Beek, F. C. Sperna Weiland, B. F. Chao, Y.-H. Wu, and M. F. P. Bierkens (2012), Past and future contribution of global groundwater depletion to sea-level rise, *Geophys. Res. Lett.*, *39*, L09402, doi:10.1029/2012GL051230.
- Walker, W. E., M. Haasnoot, and J. H. Kwakkel (2013), Adapt or perish: A review of planning approaches for adaptation under deep uncertainty, *Sustainability*, *5*(3), 955–979.
- Watkiss, P., A. Hunt, W. Blyth, and J. Dyszynski (2015), The use of new economic decision support tools for adaptation assessment: A review of methods and applications, towards guidance on applicability, *Clim. Change*, *132*(3), 401–416.
- Wilby, R. L., and S. Dessai (2010), Robust adaptation to climate change, *Weather*, *65*(7), 180–185.